IEEE Photonics Journal
An IEEE Photonics Society Publication

Open Access

Design of Compact TE-Polarized Mode-Order Converter in Silicon Waveguide With High Refractive Index Material

Volume 10, Number 6, December 2018

Danfeng Zhu
Han Ye
Zhongyuan Yu
Jing Li
Fengyi Yu
Yumin Liu

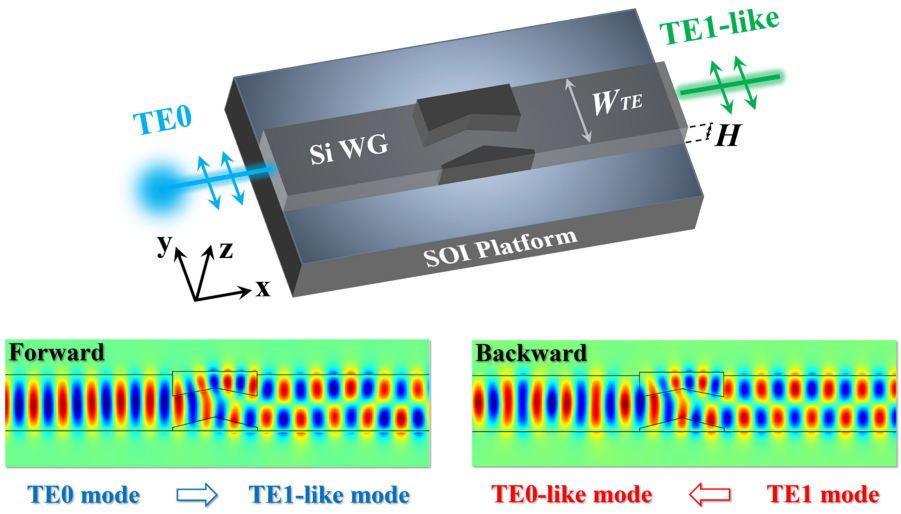

DOI: 10.1109/JPHOT.2018.2883209
1943-0655 © 2018 CCBY

Design of Compact TE-Polarized Mode-Order Converter in Silicon Waveguide With High Refractive Index Material

Danfeng Zhu, Han Ye, Zhongyuan Yu, Jing Li, Fengyi Yu, and Yumin Liu

State Key Laboratory of Information Photonics and Optical Communications, Beijing University of Posts and Telecommunications, Beijing 100876, China

DOI:10.1109/JPHOT.2018.2883209
This work is licensed under a Creative Commons Attribution 3.0 License. For more information, see http://creativecommons.org/licenses/by/3.0/

Manuscript received September 28, 2018; revised November 11, 2018; accepted November 20, 2018. Date of publication November 23, 2018; date of current version December 7, 2018. This work was supported by the National Natural Science Foundation of China under Grant 61671090 and in part by the Fund of State Key Laboratory of Information Photonics and Optical Communications, Beijing University of Posts and Telecommunications, P. R. China under Grant IPOC2017ZT07. Corresponding author: Zhongyuan Yu (e-mail: yuzhongyuan30@hotmail.com).

Abstract: We propose and numerically demonstrate a design of bidirectional transverse electric (TE) polarized mode-order converter based on silicon-on-insulator platform. This converter is realized by introducing high refractive index material inlaid in a silicon slab waveguide. Simulated by three-dimensional finite-difference time-domain method, the forward (TE0 to TE1-like conversion) transmittance reaches approximately 88.2%, while the backward value (TE1 to TE0-like conversion) is about 89.4% at the wavelength of 1550 nm. The footprint of this converter is as small as $0.95 \times 1.5\ \mu m^2$. Fabrication tolerance analysis demonstrates satisfactory robustness. Moreover, we present a polarization-independent converter with slightly modified geometry. The transmittance keeps above 87.2% within the wavelength range from 1500 nm to 1600 nm for both TE and transverse magnetic modes. These devices are expected to contribute to the on-chip mode division multiplexing.

Index Terms: Integrated optics devices, Mode conversion, Silicon waveguide.

1. Introduction

In recent years, the capacity of fiber-optic networks based on dense wavelength division multiplexing (DWDM) technology has become increasingly saturated. Space division multiplexing (SDM) technology has been confirmed as an effective solution. As an integrated SDM technique, mode division multiplexing (MDM) has caught extensive attention by introducing a novel channel for the on-chip optical communication system. Different spatial eigen-modes can be utilized as new parallel channels to encode separate data in a waveguide [1]. In photonics, the mode converter, which achieves free conversion between different modes, is a key component to conduct MDM systems [2], and attracts tremendous interest due to their potential applications in optical integrated circuits [3]–[5].

Typically, mode conversion can be divided into three types, including photonic to photonic mode, plasmonic to plasmonic mode [6]–[9], and photonic to plasmonic mode [10]–[13]. The photonic-to-photonic mode conversion mainly consists of mode-order converters and polarization rotators

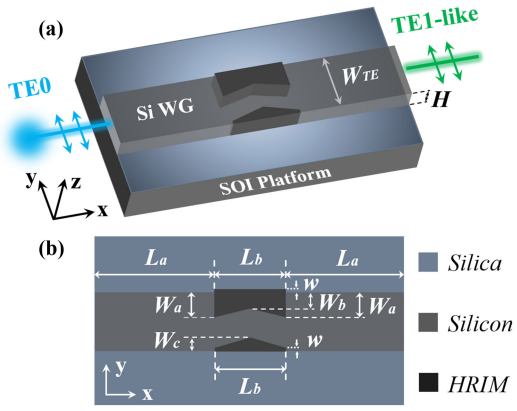

Fig. 1. (a) Three-dimensional schematics and (b) top view of the proposed TE-polarized mode-order converter.

[14]–[18]. Various schemes have been reported for the mode-order converter. For example, introducing Bragg gratings in a silicon waveguide, mode-order conversion was observed in the reflections by gratings [19], [20]. To get a higher transmission efficiency, many efforts were focused on Mach-Zender interference structures [21]–[24]. But these designs were longer than 18.5 μm. To overcome this shortcoming, photonic crystal waveguide was proved as one of the candidates [5], [25]–[27]. However, the transmission efficiency was compromised due to the coupling losses. In order to effectively reduce this adverse loss, computation-designed defects were introduced in a silicon slab waveguide by topology optimization [28]–[31]. Spatial mode conversions could be obtained by introducing dielectric or metallic metasurface on the waveguide [2], [32]. Assisted by a plasmonic splitter [33], the fundamental transverse electric (TE0) mode was perfectly converted to the first-order transverse electric (TE1) mode with a 100-nm operational bandwidth. By etching two nanowires in a silicon slab waveguide, a TE0-to-TE1 mode converter was realized with over 200-nm operational bandwidth [34]. A fundamental-to-high-order transverse magnetic (TM) mode conversions were obtained in a waveguide structure with zero index metamaterials with air grooves [35]. However, most of the above devices are full of challenges for traditional complementary metal oxide semiconductor (CMOS) processes. In short, there is plenty room for improvements such as footprint. Still, ideal schemes with low insertion loss, large operational bandwidth, high mode purity, and ease of fabrication are pursued.

Here, we propose a novel TE-polarized mode-order converter by introducing high refractive index material (HRIM) inlaid in a silicon multimode waveguide. This design is aimed for TE0-to-TE1 conversion. We conduct systematic investigations on the robustness of fabrication error. Moreover, a polarization-independent mode conversion is demonstrated. These devices are all focused on the telecommunication wavelength around 1550 nm.

2. Device Design

The schematic configuration of the proposed TE-polarized mode-order converter is depicted in Fig. 1(a). We introduce HRIM inlaid in a silicon slab waveguide. The functional region is composed of three parts: the upper HRIM area, the middle silicon waveguide, and the lower HRIM area. As shown in Fig. 1(b), the upper and lower HRIM areas both consist of two mirrored right angle trapezoids. The functional region has the symmetry with respect to the y-axis. We locate 3 μm-long silicon waveguides at each side of the functional region. The geometric parameters of the model are listed in Table 1.

Three-dimensional finite-difference time-domain (3D FDTD) method is adopted to calculate the performance of the mode converter based on silicon-on-insulator (SOI) platform. There is no upper cladding material but air is supposed. A mode source is placed in the waveguide and the model

TABLE 1
Geometric Parameters of the TE Mode-Order Converter

TE0-TE1	H	L_a	L_b	W_a	W_b	W_c	W_{TE}	w
Value (nm)	340	3000	1500	350	230	230	900	50

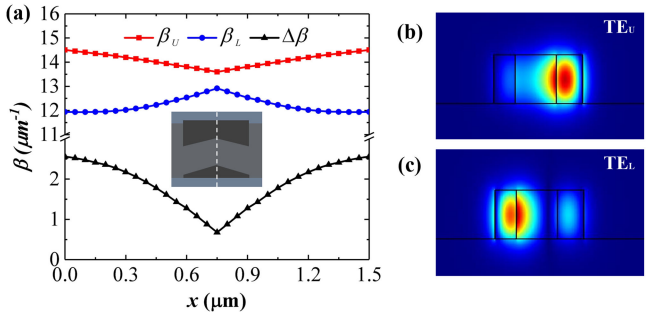

Fig. 2. (a) Propagation constants of modes in functional region. (b) Upper and (c) lower eigen-modes supported by the TE-polarized mode-order converter at the middle ($x = 0.75$) of functional region.

is surrounded by perfectly matched layers (PMLs) in the simulation. The refractive indices of silica and silicon are set as $n(Silica) = 1.44$ and $n(Silicon) = \sqrt{12}$, respectively [36]. As described, we introduce regular shaped HRIM inlaid in upper and lower areas of a silicon slab waveguide. Such design is aimed to form two paths for light and simultaneously introduces proper phase shift between them within the functional region, which are two important factors of mode conversion between TE0 and TE1. We set refractive index of HRIM as value $n = n(Silicon) + \Delta n$ ($\Delta n = 0.8$). GeSi alloy may be a suitable choice of HRIM [37]–[40]. Due to bevels of the HRIM, the propagation constant of the waveguide varies along the wave propagation direction. Therefore, we perform eigen-mode analysis with a step of 50 nm along x-axis. Fig. 2(b) and 2(c) show that the proposed converter supports two eigen-modes with their electric fields mainly localized at the upper (Fig. 2(b), named TE$_U$) and lower (Fig. 2(c), named TE$_L$) functional region. The electric fields of TE$_U$ and TE$_L$ indicate the functional region can gradually divide the input beam (TE0) into two. The propagation constants of these two modes are illustrated in Fig. 2(a). The propagation constant difference can be fitted by a simple quadratic polynomial $\Delta\beta = ax^2 + bx + c$, where a, b, and c are respectively -2.66, -0.54, and 2.56. The total shift can be roughly estimated by $\Delta\varphi = \int_0^l \Delta\beta dx = 2\int_0^{l/2} (ax^2 + bx + c)dx$, where $l = 1.5$ μm is the length of functional region. The phase shift is approximate 0.9 π at the wavelength of 1550 nm. The calculated phase shift gets close to π, indicating the possibility of TE0-to-TE1 mode conversion in the proposed design.

3. Results and Discussion

In 3D simulations, the electric fields (E_y) at 1550 nm are depicted in Fig. 3. When the TE0 mode is excited at the left port of multimode silicon waveguide in Fig. 3(a), part of the light gradually couples into the upper HRIM area. The remaining light couples in the middle silicon and lower HRIM area. Since the refractive index of HRIM is higher than that of silicon, the propagation constant of the upper HRIM region outstrips that of the middle silicon and the lower HRIM region. So phase difference of these two modes is introduced in the functional region. As discussed previously, the collective phase shift approaches to π. Consequently, the TE0 mode is converted to the TE1-like mode in the forward direction. Since this design does not have two explicitly separated paths, weak interference between two modes are inevitable. When the TE1 mode is excited at the right port of multimode silicon waveguide in Fig. 3(b), the TE1 mode is converted to the TE0-like mode due to

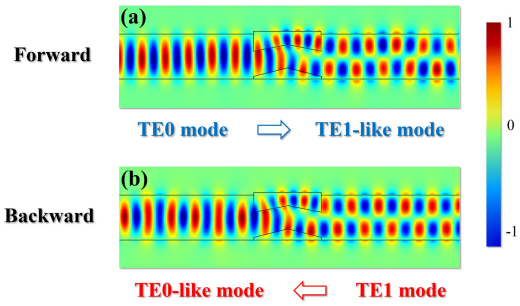

Fig. 3. Electric field profile E_y in (a) forward direction and (b) backward direction.

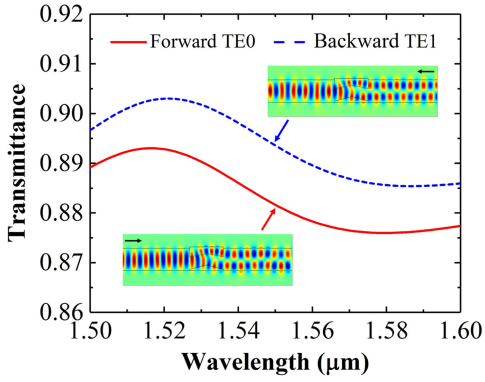

Fig. 4. Transmittance of the TE-polarized mode-order converter.

the reciprocity of the Lorentz theorem [41]. The proposed converter possesses small footprint of $0.95 \times 1.5\ \mu m^2$. It is certainly beneficial to high-density photonic integration.

For a mode converter in waveguide, high transmittance (low insertion loss) is important. Fig. 4(a) illustrates the transmittance of the proposed TE-polarized mode-order converter. The red solid line represents the forward transmittance (input TE0) while the blue dotted line represents the backward transmittance (input TE1). The TE0 mode is excited and converted to the TE1-like mode with a high transmittance of 88.2% at 1550 nm in forward direction. Meanwhile, the transmittance keeps above 87.6% within the wavelength range from 1500 nm to 1600 nm. Moreover, when the TE1 mode is excited and propagates in backward direction, the transmittance of output TE0-like mode is as high as 89.4% at 1550 nm. In the 100-nm operational bandwidth, the transmittance keeps above 88.5% and reaches highest 90.3% near 1520 nm. It can be seen the shapes of the red solid line and the blue dotted line are almost identical. The small deviation from the expected time-reversal symmetry is supposed deriving from the imperfection of mode conversion between TE0 and TE1.

When the refractive index of HRIM is changed, parameters W_a, W_b, and W_c must be modified in order to maintain the functionality of the converter as shown in Fig. 5(a). The modified parameters are listed in Table 2. As $\triangle n$ increases, W_a and W_b tend to decrease while W_c tends to increase. When $\triangle n$ ranges from 0.7 to 0.9, the transmittances keep above 87.6% within the 100-nm operational bandwidth. Redshift of the transmittance peak is observed with increasing $\triangle n$. In addition, considering the existence of experimental fabrication errors, tolerance analysis is implemented. Four possibly sensitive situations are taken into account as shown in Figs. 5(b–e). When the deviations of W_a, W_b, and W_c are respectively within 10 nm, the transmittances all keep over 84.7%. The performance of the device has not been substantially affected. Then, we consider the situation when the tip of HRIM is chopped and the bevels of HRIM are trapezoidal. It is obvious that the performance of the device is stable as shown in Fig. 5(e). At last, we simulate the situation when materials are dispersive and germanium is used as HRIM. The wavelength-dependent complex relative

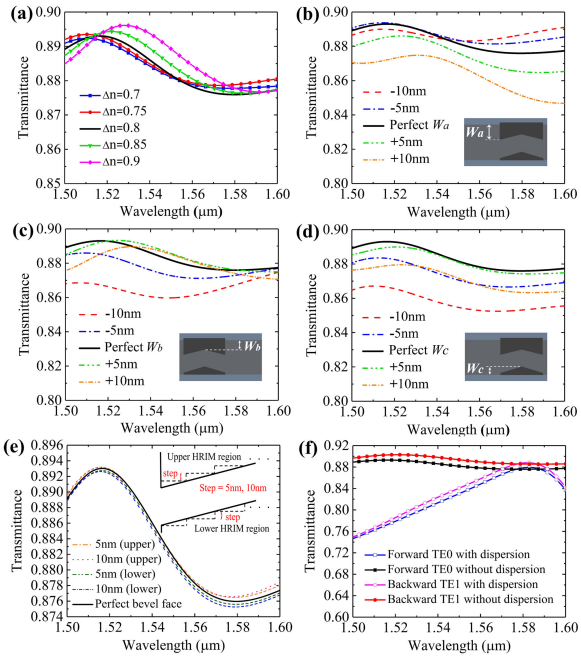

Fig. 5. Fabrication tolerance analysis of the TE-polarized mode-order converter. (a) Refractive index of HRIM. (b) Parameter W_a of the upper HRIM region. (c) Parameter W_b of the upper HRIM region. (d) Parameter W_c of the lower HRIM region. (e) Trapezoidal bevels of the upper and lower HRIM regions. (f) Materials are dispersive and germanium is used as HRIM.

TABLE 2
Modified Parameters of the TE Mode-Order Converter With Different △n

Δn	**0.7**	**0.75**	**0.8**	**0.85**	**0.9**
W_a (nm)	360	350	350	330	310
W_b (nm)	310	250	230	220	220
W_c (nm)	230	230	230	240	240

permittivity of germanium is fitted based on the Palik data. Due to the dispersion and loss of germanium, the forward (input TE0) transmittance is reduced to 83.2% while the backward (input TE1) value is about 84.1% at 1550 nm, as shown in Fig. 5(f). The performance of the TE-polarized mode-order converter is not compromised. Therefore, this converter possesses satisfactory robustness.

Finally, we present a polarization-independent converter as shown in Fig. 6(a). The height of the silicon slab waveguide is also set as 340 nm. The functional region is similarly composed of three parts: the upper HRIM area, the middle silicon waveguide and the lower HRIM area. The functional region is symmetrical about the *y*-axis as well. Based on the design of above TE-polarized mode-order converter, we modify three structural parameters of the upper and lower HRIM and the width of the silicon slab waveguide. The geometric parameters of this device are listed in Table 3. At the expense of mode purity in TE0-to-TE1 conversion, we strike a balance between TE0-to-TE1 and TM0-to-TM1 conversions. Fig. 6(b) depicts the transmittances of the TE and TM modes. When TE0 (TE1) mode is excited at the left port of multimode silicon waveguide, the transmittance reaches 89.5% (90.6%) at 1550 nm. For TM0 and TM1 mode excited at the left port, the transmittances are approximately 88.1% and 88.9%, respectively. The transmittance keeps above 87.2% with the

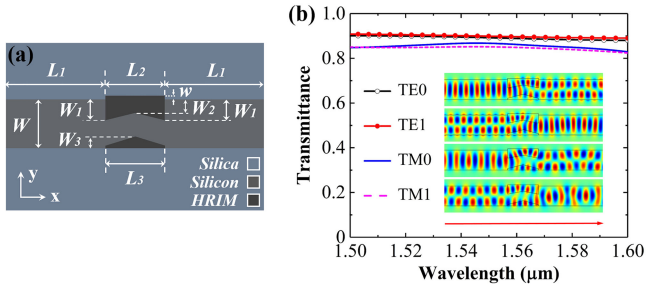

Fig. 6. (a) Schematics of the proposed polarization-independent converter. (b) Transmittances of the TE and TM mode. The insets are the electric fields when the TE0, TE1, TM0, and TM1 mode are respectively excited at the left port of multimode silicon waveguide.

TABLE 3
Geometric Parameters of the Polarization-Independent Converter

Parameter	L_1	L_2	W_1	W_2	W_3	W	w
Value (nm)	3000	1500	350	230	230	850	50

wavelength range from 1500 nm to 1600 nm for both TE and TM modes. The corresponding electric fields are illustrated in Fig. 6(b). It can be seen that both conversions are acceptable.

4. Conclusion

In conclusion, we have proposed a design of bidirectional TE-polarized mode-order converter by introducing HRIM in silicon slab waveguide. The conversion between TE0 mode and TE1-like mode is achieved within a compact functional region whose footprint is $0.95 \times 1.5\ \mu m^2$. When the TE0 (TE1) mode is incident at the left (right) port, the transmittance reaches approximately 88.2% (89.4%) at 1550 nm. More importantly, fabrication tolerance analysis is implemented for several geometric parameters. The transmittance of the proposed device keeps above 84.7% within 10-nm fabrication errors. The simulation results demonstrate the converter possesses acceptable robustness. Moreover, we present a polarization-independent mode-order converter with slight modification. The transmittance of input TE0, TE1, TM0, and TM1 are 89.5%, 90.6%, 88.1%, and 88.9% at 1550 nm, respectively. We expect these compact designs in silicon slab waveguide contribute to the integrated MDM systems.

References

[1] R. Kirchain and L. Kimerling, "A roadmap for nanophotonics," *Nature Photon.*, vol. 1, no. 6, pp. 303–305, Jun. 2007.
[2] D. Ohana, D. Boris, N. Mazurski, and U. Levy, "Dielectric metasurface as a platform for spatial mode conversion in nanoscale waveguides," *Nano Lett.*, vol. 16, no. 12, pp. 7956–7961, Dec. 2016.
[3] V. R. Almeida, C. A. Barrios, R. R. Panepucci, and M. Lipson, "All-optical control of light on a silicon chip," *Nature*, vol. 431, no. 7012, pp. 1081–1084, Oct. 2004.
[4] L. H. Gabrielli, D. Liu, S. G. Johnson, and M. Lipson, "On-chip transformation optics for multimode waveguide bends," *Nature Commun.*, vol. 3, Nov. 2012, Art. no. 1217.
[5] H. Ye, D. Wang, Z. Yu, J. Zhang, and Z. Chen, "Ultra-compact broadband mode converter and optical diode based on linear rod-type photonic crystal waveguide," *Opt. Exp.*, vol. 23, no. 8, pp. 9673–9680, Apr. 2015.
[6] Y. T. Hung, C. B. Huang, and J. S., Huang, "Plasmonic mode converter for controlling optical impedance and nanoscale light-matter interaction," *Opt. Exp.*, vol. 20, no. 18, pp. 20342–20355, Aug. 2012.
[7] S. An *et al.*, "Nanofocusing of light using three-dimensional plasmonic mode conversion," *Opt. Exp.*, vol. 21, no. 23, pp. 27816–27825, Nov. 2013.

[8] W. H. Dai, F. C. Lin, C. B. Huang, and J. S. Huang, "Mode conversion in high-definition plasmonic optical nanocircuits," *Nano Lett.*, vol. 14, no. 7, pp. 3881–3886, Jul. 2014.
[9] V. F. Nezhad, A. Haddadpour, and G. Veronis, "Tunable spatial mode converters and optical diodes for graphene parallel plate waveguides," *Opt. Exp.*, vol. 24, no. 21, pp. 23883–23897, Oct. 2016.
[10] A. Melikyan, M. Kohl, M. Sommer, C. Koos, W. Freude, and J. Leuthold, "Photonic-to-plasmonic mode converter," *Opt. Lett.*, vol. 39, no. 12, pp. 3488–3491, Jun. 2014.
[11] R. Yang, R. A. Wahsheh, Z. L. Lu, and M. A. G. Abushagur, "Efficient light coupling between dielectric slot waveguide and plasmonic slot waveguide," *Opt. Lett.*, vol. 35, no. 5, pp. 649–651, Mar. 2010.
[12] T. Srivastava, R. Das, and R. J. Jha, "Mode-coupling between surface plasmon modes and bandgap-guided modes: A comprehensive study and applications," *J. Lightw. Technol.*, vol. 31, no. 22, pp. 3518–3524, Nov. 2013.
[13] S.-Y. Lee, J. Kim, I.-M. Lee, and B. Lee, "Efficient transition between photonic and plasmonic guided modes at abrupt junction of MIM plasmonic waveguide," *Opt. Exp.*, vol. 21, no. 18, pp. 20762–20770, Sep. 2013.
[14] S. An and O. K. Kwon, "Integrated InP polarization rotator using the plasmonic effect," *Opt. Exp.*, vol. 26, no. 2, pp. 1305–1314, Jan. 2018.
[15] W. F. Jiang, "Fabrication-tolerant polarization splitter and rotator based on slanted silicon waveguides," *IEEE Photon. Technol. Lett.*, vol. 30, no. 7, pp. 614–617, Apr. 2018.
[16] H. C. Chung and S. Y. Tseng, "Ultrashort and broadband silicon polarization splitterrotator using fast quasiadiabatic dynamics," *Opt. Exp.*, vol. 26, no. 8, pp. 9655–9665, Apr. 2018.
[17] Y. Zhang, Y. J. Feng, and T. Jiang, "Tunable broadband polarization rotator in terahertz frequency based on graphene metamaterial," *Carbon*, vol. 133, pp. 170–175, Jul. 2018.
[18] H. N. Xu, L. Liu, and Y. C. Shi, "Polarization-insensitive four-channel coarse wavelength-division (de)multiplexer based on mach-zehnder interferometers with bent directional couplers and polarization rotators," *Opt. Lett.*, vol. 43, no. 7, pp. 1483–1486, Apr. 2018.
[19] J. M. Castro and D. F. Geraghty, "Demonstration of mode conversion using anti-symmetric waveguide Bragg gratings," *Opt. Exp.*, vol. 13, no. 11, pp. 4180–4184, May. 2005.
[20] H. Y. Qiu *et al.*, "Silicon mode multi/demultiplexer based on multimode grating-assisted couplers," *Opt. Exp.*, vol. 21, no. 15, pp. 17904–17911, Jul. 2013.
[21] B. T. Lee and S. Y. Shin, "Mode-order converter in a multimode waveguide," *Opt. Exp.*, vol. 28, no. 18, pp. 1660–1662, Sep. 2003.
[22] Y. Huang, G. Xu, and S.-T. Ho, "An ultracompact optical mode order converter," *IEEE Photon. Technol. Lett.*, vol. 18, no. 21, pp. 2281–2283, Nov. 2006.
[23] A. Hosseini, J. Covey, and R. T. Chen, "Mode order converter using tapered multi-mode interference couplers," in *Proc. Integr. Photon. Res., Silicon Nanophotonics*, 2010, Paper IWB2.
[24] D. G. Chen, X. Xi, L. Wang, Y. Yu, W. Liu, and Q. Yang, "Low-loss and fabrication tolerant silicon mode order converters based on novel compact tapers," *Opt. Exp.*, vol. 23, no. 9, pp. 11152–11159, May 2015.
[25] V. Liu, D. A. B. Miller, and S. H. Fan, "Ultra-compact photonic crystal waveguide spatial mode converter and its connection to the optical diode effect," *Opt. Exp.*, vol. 20, no. 27, pp. 28388–28397, Dec. 2012.
[26] L. H. Frandsen *et al.*, "Topology optimized mode conversion in a photonic crystal waveguide fabricated in siliconon-insulator material," *Opt. Exp.*, vol. 22, no. 7, pp. 8525–8532, Apr. 2014.
[27] H. Ye, Z. Y. Yu, Y. M. Liu, and Z. H. Chen, "Realization of compact broadband optical diode in linear air-hole photonic crystal waveguide," *Opt. Exp.*, vol. 24, no. 21, pp. 24592–24599, Oct. 2016.
[28] J. Lu and J. Vučković, "Objective-first design of high-efficiency, small-footprint couplers between arbitrary nanophotonic waveguide modes," *Opt. Exp.*, vol. 20, no. 7, pp. 7221–7236, Mar. 2012.
[29] L. F. Frellsen, Y. H. Ding, O. Sigmund, and L. H. Frandsen, "Topology optimized mode multiplexing in silicon-on-insulator photonic wire waveguides," *Opt. Exp.*, vol. 24, no. 15, pp. 16866–16873, Jul. 2016.
[30] F. Callewaert, S. Butun, Z. Y. Li, and K. Aydin, "Inverse design of an ultra-compact broadband optical diode based on asymmetric spatial mode conversion," *Scientific Reports*, vol. 6, Sep. 2016, Art. no. 32577.
[31] W. J. Chang *et al.*, "Ultra-compact mode (de)multiplexer based on subwavelength asymmetric Y-junction," *Opt. Exp.*, vol. 26, no. 7, pp. 8162–8170, Apr. 2018.
[32] Z. Y. Li *et al.*, "Controlling propagation and coupling of waveguide modes using phase-gradient metasurfaces," *Nature Nanotechnol.*, vol. 12, no. 7, p. 675, Jul. 2017.
[33] J. Li, H. Ye, Z. Y. Yu, and Y. M. Liu, "Design of a broadband reciprocal optical diode in a silicon waveguide assisted by silver surface plasmonic splitter," *Opt. Exp.*, vol. 25, no. 16, pp. 19129–19136, Jul. 2017.
[34] W. M. Ye, X. D. Yuan, Y. Gao, and J. L. Liu, "Design of broadband silicon-waveguide mode-order converter and polarization rotator with small footprints," *Opt. Exp.*, vol. 25, no. 26, pp. 33176–33183, Dec. 2017.
[35] E. Qian, Y. Y. Fu, and Y. D. Xu, "Perfect waveguide mode conversion via zero index metamaterials," *J. Optics*, vol. 19, no. 1, Jan. 2017, Art. no. 015102.
[36] D. F. Zhu, J. Q. N. Zhang, H. Ye, Z. Y. Yu, and Y. M. Liu, "Design of a broadband reciprocal optical diode in multimode silicon waveguide by partial depth etching," *Opt. Commun.*, vol. 418, pp. 88–92, Jul. 2018.
[37] E. S. Y. El-Zaiat and G. M. Youssef, "Dispersive parameters for complex refractive index of p- and n-type silicon from spectrophotometric measurements in spectral range 200-2500 nm," *Opt. Laser Technol.*, vol. 65, pp. 106–112, Jan. 2015.
[38] H. H. Hulkkonen, T. Salminen, and T. Niemi, "Block copolymer patterning for creating porous silicon thin films with tunable refractive indices," *ACS Appl. Mater. Interfaces*, vol. 9, no. 37, pp. 31260–31265, Sep. 2017.
[39] R. Claps, V. Raghunathan, O. Boyraz, P. Koonath, D. Dimitropoulos, and B. Jalali, "Raman amplification and lasing in SiGe waveguides," *Opt. Exp.*, vol. 13, no. 7, pp. 2459–2466, Apr. 2005.
[40] F. Schaffler, *Properties of Advanced Semiconductor Materials: GaN, AlN, InN, BN, SiC, SiGe*. Hoboken, NJ, USA: Wiley, 2001.
[41] D. Jalas *et al.*, "What is—and what is not—an optical isolator," *Nature Photon.*, vol. 7, no. 8, pp. 579–582, Aug. 2013.